

PCA Regularized Nonrigid Registration for PET/MRI Attenuation Correction

Volker Daum^{1,2}, Dieter A. Hahn¹, Joachim Hornegger^{1,3}, and Torsten Kuwert⁴

¹ Chair of Pattern Recognition, Friedrich-Alexander University Erlangen-Nürnberg (FAU), Erlangen, Germany

² Institute of Optics, Information and Photonics (Max-Planck Research Group), FAU

³ Erlangen Graduate School in Advanced Optical Technologies (SAOT), Erlangen, Germany

⁴ Department of Nuclear Medicine, University Hospital, FAU

Abstract. An open issue in the use of hybrid PET / MRI scanners is the attenuation correction of the PET image. In order to solve this problem, we propose to perform a nonrigid registration of an atlas CT image with the MRI. The registered atlas CT contains the information about the tissue densities necessary for the attenuation correction.

In multi-modal, nonrigid image registration, the correspondence between the intensity values is not known a priori. Statistical, multi-modal distance measures determine this correspondence during the registration solely from the intensity distributions. Without the incorporation of prior knowledge this may lead to wrong results, such as the alignment of the skull with brain tissue, or the skin with fat surrounding the skull. Therefore, we propose a novel, PCA-based regularization of the nonrigid registration. This limits the possible registration results to morphologically plausible deformations. The model is constructed such that it is invariant to global translations in the registration. Thus, the registration is less dependent on the initial, rigid preregistration.

Results are presented on a database of 18 CT datasets for the training of a PCA deformation model. MR images of the same patients have been rigidly registered with the corresponding CT datasets, which are used as ground truth for the tests. The evaluation is performed using a leave-one-out cross-validation by registering an atlas onto the total of 38 MRI datasets and comparing the deformed atlas with the ground truth CT of the patient. Results indicate a better performance of the proposed approach compared to the standard. On average, the mean squared error is decreased by 18% and the sensitivity for correct soft tissue and bone alignment is increased by 4%.

1 Introduction

The advent of hybrid scanners, for example the combination of PET (Positron Emission Tomography) and CT (Computed Tomography) imaging within one machine, has brought many new possibilities to the field of medical imaging, such as the invention of highly specific tumor markers. However, the superior

tissue contrast and the large variety of different sequences offered by MRI make it desirable to replace the CT with an MRI (Magnetic Resonance Imaging) scanner in such hybrid systems. Although there are still technical difficulties to overcome, first combined PET / MRI scanners for acquisition of the human head have already been built, and it is only a matter of time until they enter the market.

One of the difficulties to overcome in PET / MRI hybrid scanners is the attenuation correction of the PET image. In PET, the aim is to measure the concentration of a radioactive marker within the patient body. The quantity that the machine can actually measure is the radiation emitted by the tracer. The rays are attenuated by the anatomical structures while traveling through the human body. Therefore, it is necessary to provide an attenuation map for each acquisition in order to perform an attenuation correction of the dose measured in the PET image. The map can be created, for instance, from a CT, where the relation between the intensities within the image and the tissue densities is known.

The values measured by MRI, however, are not related to the attenuation, therefore, no straightforward solution is currently available for the attenuation correction in case of a hybrid PET / MRI scanner. In the following, we propose a method based on the registration between an atlas CT and the MRI image. The deformed atlas image then replaces the missing CT of the patient and can be used for the attenuation correction.

The multi-modal, nonrigid registration, which is used to perform such an atlas registration, offers many degrees of freedom in the spatial domain. It is more difficult than the mono-modal registration, because the relation between the image intensities is not known a priori. This may lead to mis-registrations where a low value for the distance measure indicates a good alignment of the images, however, the deformation may not be correct in the physical and morphological sense. Hence, we propose a novel regularization of the nonrigid registration process that incorporates prior knowledge in terms of a deformation model. This morphologically-based regularization utilizes a PCA (Principal Component Analysis) of the previously acquired deformation fields computed from CT images of a collective of patients. These registrations performed within the CT modality use a sum-of-squared differences similarity measure. The intra-modal registrations are, in our experience, better conditioned than the multi-modal, nonrigid registrations between CT and MRI. The result of this learning phase is an atlas CT, together with a model for the variations within the deformations. This prior knowledge is used to constrain the registration between the MRI of the hybrid scanner with the atlas CT to penalize morphologically improbable deformations.

This article is organized as follows. First, we introduce related work regarding the attenuation correction, morphological models in image registration, and the nonrigid registration. The methods provide information about the registration, distance measures, and the model generation. In the final section we present a leave-one-out cross-validation of 18 CT images used for the atlas CT creation and applied to MR images, and discuss the results.

2 Related Work

A very recent survey of PET / MRI attenuation techniques can be found in [1]. Usually, the employed methods are categorized into segmentation- or classification-based approaches. In segmentation-based correction, the intensities of the MRI image are directly transformed into an attenuation map. Using an atlas for the correction, an atlas CT is transformed into the space of the MRI to provide the tissue densities. In addition, combined methods can be applied that first perform an atlas registration and use additional knowledge from the atlas to improve the results of a classification approach [2].

Statistical morphological constraints in image registration have already been employed. Wang and Staib [3] describe a method that generates a sparse PCA-based model on a set of boundary points that they use to constrain the dense nonrigid registration. Kim et. al.[4] construct a dense PCA-based deformation model from registrations with a standard registration approach. The model is used to generate a large set of sample images which are then compared to the reference image in order to find a good starting position for a standard registration approach. An alternative to a simple PCA model is proposed by Xue and Shen [5]. They, instead, use a wavelet PCA that has the advantage to also capture very local and fine grained deformations. Nevertheless, the model is only used for an initial registration followed by an unconstrained nonrigid registration.

In this work we focus on a nonrigid, nonparametric atlas registration of a CT dataset with MRI, similar to the approaches presented in [6, 7]. As distance measure we employ the mutual information (MI), based on the works of Viola [8] and Hermosillo [6]. As regularization term we employ a curvature term introduced by Fischer and Modersitzki [9].

3 Methods

In the following, we present the applied nonrigid registration framework 3.1 that is used both to generate the atlas CT, and to register the MRI with the atlas CT. In section 3.2, we describe the applied intensity distance measures, which are used as objective functions for the registration. The regularization of the registrations is based on the curvature of the deformation field 3.3, which is then supplemented by the deformation model created with the PCA on the sample deformation fields. The novel regularization approach is described in 3.4, followed by the modeling of the translation invariance 3.5.

3.1 Nonrigid Registration Framework

In nonrigid, nonparametric registration the dense deformation field \mathbf{u} is calculated between the spatial positions of each voxel. It is determined by minimizing a distance measure \mathcal{D} , which evaluates the quality of the match between the moving image M and the fixed image F . Its optimization is subject to a smoothness constraint \mathcal{S} to ensure that the resulting deformation does not contain any

cracks, ridges, or folds. This constraint is usually incorporated as a penalty term weighted by a parameter $\alpha \in \mathbb{R}_{>0}$, i.e. lower values of α will result in a less smooth deformation field, but a better match and vice versa. The optimization of the distance alone is ill-posed and the addition of the smoothness constraint is related to classical Tikhonov regularization [10]:

$$\hat{\mathbf{u}} = \underset{\mathbf{u}}{\operatorname{argmin}} \mathcal{E}(F, M, \mathbf{u}) = \underset{\mathbf{u}}{\operatorname{argmin}} \mathcal{D}(F, M_{\mathbf{u}}) + \alpha \mathcal{S}(\mathbf{u}) \quad (1)$$

$$M_{\mathbf{u}}(x) = M(x - \mathbf{u}(x))$$

The optimization problem is to find a minimizer for the functional (1) in the space of all deformation fields \mathcal{U} . If we assume that \mathcal{E} is sufficiently smooth and differentiable, and with appropriate boundary conditions, we can apply the calculus of variations to find a minimizer $\hat{\mathbf{u}}$. For the direction $\mathbf{v} \in \mathcal{U}$ of the first variation, the Gâteaux derivative of (1) is defined as:

$$\delta \mathcal{E}(F, M, \mathbf{u} \circ \mathbf{v}) = \lim_{\epsilon \rightarrow 0} \frac{\mathcal{E}(F, M, \mathbf{u} + \epsilon \mathbf{v}) - \mathcal{E}(F, M, \mathbf{u})}{\epsilon} = \left. \frac{d\mathcal{E}(F, M, \mathbf{u} + \epsilon \mathbf{v})}{d\epsilon} \right|_{\epsilon=0} \quad (2)$$

For the existence of a minimizer for (1), it is necessary that the Gâteaux derivative vanishes for all variations \mathbf{v} : $\delta \mathcal{E}(F, M, \hat{\mathbf{u}} \circ \mathbf{v}) = 0$. If \mathcal{U} is assumed to be a Hilbert space that defines a scalar product, the gradient of the functional with respect to the optimal displacement vanishes, $\nabla_{\mathcal{U}} \mathcal{E}(F, M, \hat{\mathbf{u}}) = 0$, and the minimizer is a solution to the Euler-Lagrange equations associated with this problem:

$$\nabla_{\mathcal{U}} \mathcal{E}(F, M, \mathbf{u}) = \nabla_{\mathcal{U}} \mathcal{D}(F, M_{\mathbf{u}}) + \nabla_{\mathcal{U}} \mathcal{S}(\mathbf{u}) \quad (3)$$

As solver, we employ a Newton-type method that uses a numeric approximation of the second derivative of \mathcal{D} .

3.2 Distance Measures

For the mono-modal registration between the CT images, we apply the widely known sum-of-squared differences measure. It is based on the assumption that the intensities of corresponding tissue within the two images are equal, or differ by noise at the utmost.

$$\mathcal{D}_{\text{SSD}}(F, M_{\mathbf{u}}) = \frac{1}{|\Omega|} \int_{\Omega} (M_{\mathbf{u}}(\mathbf{x}) - F(\mathbf{x}))^2 d\mathbf{x} \quad (4)$$

with Ω being the spatial domain of the overlap between F and $M_{\mathbf{u}}$.

Distance measures based on image intensity statistics are widely used for multi-modal registration tasks. Based on Shannon's theory [11], the information content within the images is measured using the entropies of the marginal PDFs

p_F and $p_{M_{\mathbf{u}}}$, and the joint PDF $\mathbf{p}_{F, M_{\mathbf{u}}}$:

$$\mathcal{H}(F) = - \int_{\mathbb{R}} p_F(f) \log p_F(f) \, df \quad (5)$$

$$\mathcal{H}(M_{\mathbf{u}}) = - \int_{\mathbb{R}} p_{M_{\mathbf{u}}}(m) \log p_{M_{\mathbf{u}}}(m) \, dm \quad (6)$$

$$\mathcal{H}(F, M_{\mathbf{u}}) = - \int_{\mathbb{R}^2} \mathbf{p}_{F, M_{\mathbf{u}}}(\mathbf{i}) \log \mathbf{p}_{F, M_{\mathbf{u}}}(\mathbf{i}) \, d\mathbf{i} \quad (7)$$

where f , m , and $\mathbf{i} = (f, m)^T$ are intensity random measures of F and M . In the following, we make use of the MI, which was introduced by Wells et. al.[12] and Maes et. al.[13]:

$$\begin{aligned} \mathcal{D}_{\text{MI}}(F, M_{\mathbf{u}}) &= -\text{MI}(F, M_{\mathbf{u}}) \\ &= \mathcal{H}(F, M_{\mathbf{u}}) - \mathcal{H}(F) - \mathcal{H}(M_{\mathbf{u}}) \\ &= \int_{\mathbb{R}^2} \mathbf{p}_{F, M_{\mathbf{u}}}(\mathbf{i}) \log \frac{\mathbf{p}_{F, M_{\mathbf{u}}}(\mathbf{i})}{p_F(f)p_{M_{\mathbf{u}}}(m)} \, d\mathbf{i} \end{aligned} \quad (8)$$

Here, $\mathcal{D}_{\text{MI}}(M_{\mathbf{u}}, F)$ is written as a distance measure, i.e. smaller values indicate a better result.

3.3 Curvature Regularizer

The choice of a suitable smoother depends on the type of application. Common regularization techniques are based on Dirichlet, elasticity, fluidal, and higher order functionals. Among the latter ones, curvature regularization is an approach that features some advantages for medical image registration [14]:

$$\mathcal{S}_{\text{CURV}}(\mathbf{u}) = \int_{\Omega} |\Delta \mathbf{u}|^2 \, d\mathbf{x} . \quad (9)$$

This regularization term does not penalize affine transformations and leads to smooth displacement fields.

3.4 PCA Regularization

To generate the proposed morphological model, a series of mono-modal registrations is performed on CT images. The images are rigidly aligned, before a nonrigid registration is employed, which yields the training deformations. The mono-modal is considered to be more robust than the multi-modal registration, especially as one has to deal with less local minima during the optimization. For n input images, the resulting sample deformation fields \mathbf{w}_i with $i = 1, \dots, n$ are then used to extract the mean deformation and the principal modes of variation

by means of a PCA.

$$\begin{aligned}
\bar{\mathbf{w}} &= \frac{1}{n} \sum_{i=1}^n \mathbf{w}_i \\
\mathbf{W} &= ((\mathbf{w}_1 - \bar{\mathbf{w}}), \dots, (\mathbf{w}_n - \bar{\mathbf{w}})) \\
\mathbf{W}\mathbf{W}^T \mathbf{v}_i &= \lambda_i \mathbf{v}_i \\
\text{s.t. } |\mathbf{v}_i|^2 &= 1
\end{aligned} \tag{10}$$

where $\bar{\mathbf{w}}$ denotes the mean, and $\mathbf{W}\mathbf{W}^T$ the covariance matrix of the deformation. The Eigenvalue / Eigenvector decomposition of $\mathbf{W}\mathbf{W}^T$ (10) is performed as described in Murase and Lindenbaum [15]. The resulting Eigenvectors \mathbf{v}_i form an orthonormal vector space, which is an important property for the following article. Choosing the m components with the largest Eigenvalues λ_i and arranging them in a matrix \mathbf{V} our model consists of the components $\bar{\mathbf{w}}$ and $\mathbf{V} = (\mathbf{v}_1, \dots, \mathbf{v}_m)$. Using this model, the registration energy (1) is then supplemented by an additional regularization term \mathcal{P} , which enforces the result to be close to the model space.

$$\begin{aligned}
\min_{\mathbf{u}} \mathcal{E}(F, M, \mathbf{u}) &= \mathcal{D}(F, M_{\mathbf{u}}) + \alpha \mathcal{S}(\mathbf{u}) + \beta \mathcal{P}(\mathbf{u}) \\
\mathcal{P}(\mathbf{u}) &= \frac{1}{s} (\mathbf{u} - (\bar{\mathbf{w}} + \mathbf{V}\mathbf{V}^T(\mathbf{u} - \bar{\mathbf{w}})))^2 \\
&= \frac{1}{s} ((\mathbf{I} - \mathbf{V}\mathbf{V}^T)(\mathbf{u} - \bar{\mathbf{w}}))^2
\end{aligned} \tag{11}$$

where β is again a weighting factor that governs the strictness with which the morphological model is applied, and s is a normalization factor equal to the number of voxels in the images. In $\mathcal{P}(\mathbf{u})$, we measure the squared difference between \mathbf{u} and its projection onto the PCA model. Thus, $\mathcal{P}(\mathbf{u})$ quadratically penalizes a deviation from the model. For the optimization, the derivative of the new energy term \mathcal{P} is calculated as

$$\begin{aligned}
\nabla_{\mathbf{u}} \mathcal{P}(\mathbf{u}) &= \frac{2}{s} (\mathbf{I} - \mathbf{V}\mathbf{V}^T)^T (\mathbf{I} - \mathbf{V}\mathbf{V}^T) (\mathbf{u} - \bar{\mathbf{w}}) \\
&= \frac{2}{s} (\mathbf{I} - 2\mathbf{V}\mathbf{V}^T + \underbrace{\mathbf{V}\mathbf{V}^T\mathbf{V}\mathbf{V}^T}_{=\mathbf{I}}) (\mathbf{u} - \bar{\mathbf{w}}) \\
&= \frac{2}{s} (\mathbf{I} - \mathbf{V}\mathbf{V}^T) (\mathbf{u} - \bar{\mathbf{w}})
\end{aligned} \tag{12}$$

The identity $\mathbf{V}^T\mathbf{V} = \mathbf{I}$ is due to the orthonormality of \mathbf{V} . The calculation of $\nabla_{\mathbf{u}} \mathcal{P}$ is thus very closely related to calculating \mathcal{P} itself, which saves a lot of computational complexity.

3.5 Translation Invariance

For the generation of the model, as well as its application, the datasets were aligned by a rigid registration. This is a necessary step for the usage of PCA

models, because they are, in general, dependent on a consistent initial positioning. Even though the used rigid registration performed very well, it did not always yield consistent results in the translational alignment. This is mostly due to the variation in the data for inter-patient registration cases. For example, when the facial bone between two datasets matches very well, the rigid registration will tend to align it, and, if the back of the skulls is morphologically similar, the rigid registration is likely to match this part best. The rotation did generally not suffer from these problems. A successful nonrigid registration might incorporate these inconsistencies into the deformation model, which then leads to problems later in the application stage.

To overcome these inconsistencies in the preregistration, we introduce a deformation model in the following that is invariant to global translations, i.e. global translations in a vector field will neither be learned nor penalized. In order to do this, the global translation is removed from the training data. Nonetheless, the global translation can still be incorporated by augmenting the PCA model with additional basis vectors for the global translation.

Let the vector field \mathbf{u} be organized in the components of the coordinate system (x, y, z) :

$$\mathbf{u} = \underbrace{(u_1, \dots, u_s)}_{x \text{ components}}, \underbrace{(u_{s+1}, \dots, u_{2s})}_{y \text{ components}}, \underbrace{(u_{2s+1}, \dots, u_{3s})}_{z \text{ components}}^T \quad (13)$$

The calculation of the global translation $\mathbf{t}(\mathbf{u})$ can be written as a matrix vector product:

$$\begin{aligned} \mathbf{e}_0 &= (0, \dots, 0)^T \in \mathbb{R}^s \\ \mathbf{e}_1 &= \frac{1}{\sqrt{s}}(1, \dots, 1)^T \in \mathbb{R}^s \\ \mathbf{b}_x &= \begin{pmatrix} \mathbf{e}_1 \\ \mathbf{e}_0 \\ \mathbf{e}_0 \end{pmatrix} \in \mathbb{R}^{3s} & \mathbf{b}_y &= \begin{pmatrix} \mathbf{e}_0 \\ \mathbf{e}_1 \\ \mathbf{e}_0 \end{pmatrix} \in \mathbb{R}^{3s} & \mathbf{b}_z &= \begin{pmatrix} \mathbf{e}_0 \\ \mathbf{e}_0 \\ \mathbf{e}_1 \end{pmatrix} \in \mathbb{R}^{3s} \\ \mathbf{B} &= (\mathbf{b}_x, \mathbf{b}_y, \mathbf{b}_z) \\ \mathbf{t}(\mathbf{u}) &= \mathbf{B}\mathbf{B}^T \mathbf{u} \end{aligned} \quad (14)$$

where the vectors $\mathbf{b}_x, \mathbf{b}_y, \mathbf{b}_z$ describe a global translation along the corresponding coordinate axis. They are mutually orthogonal and normalized to $|\mathbf{b}_{[x,y,z]}| = 1$. Accordingly the model is generated with the modified samples

$$\begin{aligned} \tilde{\mathbf{w}}_i &= \mathbf{w}_i - \mathbf{t}(\mathbf{w}_i) \\ &= \mathbf{w}_i - \mathbf{B}\mathbf{B}^T \mathbf{w}_i \end{aligned} \quad (15)$$

and the mean of the modified samples

$$\bar{\mathbf{w}} = \frac{1}{n} \sum_{i=0}^n \tilde{\mathbf{w}}_i \quad (16)$$

The new sample vectors $\tilde{\mathbf{w}}_i$ are therefore orthogonal to the vectors $\mathbf{b}_{[x,y,z]}$ that compose \mathbf{B} .

$$\begin{aligned}\mathbf{B}^T \tilde{\mathbf{w}}_i &= \mathbf{B}^T (\mathbf{w}_i - \mathbf{B}\mathbf{B}^T \mathbf{w}_i) \\ &= \mathbf{B}^T \mathbf{w}_i - \underbrace{\mathbf{B}^T \mathbf{B} \mathbf{B}^T}_{=\mathbf{I}} \mathbf{w}_i \\ &= 0\end{aligned}\tag{17}$$

The regularizing term is adapted in the same way, by subtracting the global translation $\mathbf{t}(\mathbf{u})$ from the current deformation field \mathbf{u} before applying the PCA model.

$$\begin{aligned}\mathcal{P}(\mathbf{u}) &= \frac{1}{s} ((\mathbf{I} - \mathbf{V}\mathbf{V}^T)(\mathbf{u} - \bar{\mathbf{w}} - \mathbf{t}(\mathbf{u})))^2 \\ &= \frac{1}{s} ((\mathbf{I} - \mathbf{V}\mathbf{V}^T)(\mathbf{u} - \bar{\mathbf{w}} - \mathbf{B}\mathbf{B}^T \mathbf{u}))^2\end{aligned}\tag{18}$$

$$= \frac{1}{s} ((\mathbf{I} - \mathbf{V}\mathbf{V}^T)(\mathbf{I} - \mathbf{B}\mathbf{B}^T)(\mathbf{u} - \bar{\mathbf{w}}))^2\tag{19}$$

$$= \frac{1}{s} ((\mathbf{I} - \mathbf{V}\mathbf{V}^T - \mathbf{B}\mathbf{B}^T)(\mathbf{u} - \bar{\mathbf{w}}))^2\tag{20}$$

$$= \frac{1}{s} ((\mathbf{I} - \tilde{\mathbf{V}}\tilde{\mathbf{V}}^T)(\mathbf{u} - \bar{\mathbf{w}}))^2\tag{21}$$

$$\tilde{\mathbf{V}} = (\tilde{\mathbf{v}}_1, \dots, \tilde{\mathbf{v}}_m, \mathbf{b}_x, \mathbf{b}_y, \mathbf{b}_z)$$

The step from (18) to (19) is possible because $\bar{\mathbf{w}}$ is a linear combination of $\tilde{\mathbf{w}}_i$, which means that $\bar{\mathbf{w}}$ is orthogonal to \mathbf{B} (i.e. $\mathbf{B}\mathbf{B}^T \bar{\mathbf{w}} = 0$) due to (17). The same argument can be applied to the step from (19) to (20): the components \mathbf{v}_i of \mathbf{V} are linear combinations of the training vectors $\tilde{\mathbf{w}}_i$ and, accordingly, orthogonal to the vectors $\mathbf{b}_{[x,y,z]}$ of \mathbf{B} . Therefore, the product $\mathbf{V}\mathbf{V}^T \mathbf{B}\mathbf{B}^T = 0$. Essentially, the whole process of eliminating the global translation in the calculation of \mathcal{P} yields a new basis $\tilde{\mathbf{V}}$ by augmenting the principal components \mathbf{V} artificially with the vectors $\mathbf{b}_{[x,y,z]}$. Note that $\tilde{\mathbf{V}}$ is still orthonormal, which allows the calculation of the derivative of \mathcal{P} exactly as in (12).

$$\nabla_{\mathbf{u}} \mathcal{P}(\mathbf{u}) = \frac{2}{s} (\mathbf{I} - \tilde{\mathbf{V}}\tilde{\mathbf{V}}^T)(\mathbf{u} - \bar{\mathbf{w}})\tag{22}$$

4 Results

For an evaluation of the proposed approach, 18 CT datasets were used for the training of the model consisting of the mean deformation and the first 10 components of the PCA. The algorithm was then applied to 23 T1- and 15 T2-weighted MRI scans from the same patients in a leave-one-out cross validation. Prior to the experiments, the tables present within the CT images have been segmented and ignored during the segmentation. The CT and MRI of the same patient were rigidly registered in order to provide a ground-truth CT for every patient's

MRI dataset. This rigidly registered, ground-truth CT was used, in combination with the deformed atlas CT, to calculate objective quality measurements for the nonrigid atlas registration results. All patient data was resampled to a common volume size of $129 \times 129 \times 104$ voxels and an isotropic spacing of 1.95 mm in order to simplify model generation and evaluation.

Regarding the choice of the α parameter, please note that our algorithm operates in physical space and not on a unit square, or with a unit spacing. Intensity values were also taken into account without any rescaling. The weights for the regularizing terms can, therefore, differ from the values presented in the related work. For the generation of the training deformations, the mono-modal, nonrigid registration that uses the sum-of-squared-differences measure was regularized with a weighting factor of $\alpha = 0.01$. The multi-model registration was driven by the MI distance measure and carried out with and without the PCA regularization. With the PCA regularization enabled, the weighting factors were chosen as $\alpha = 7$ and $\beta = 0.01$. This choice represents a rather low value for α and would result in very large local deformations without the additional morphological regularization. An example of this setting is shown in Fig. 1. Here

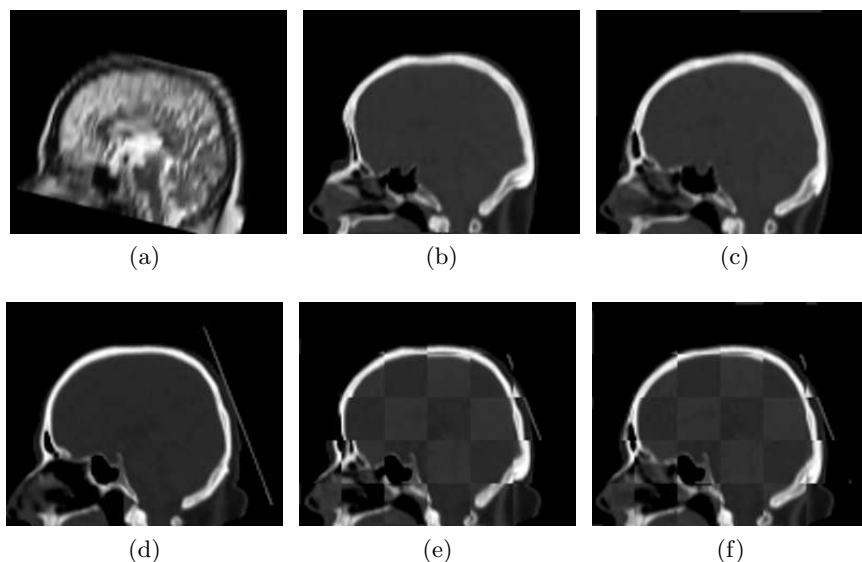


Fig. 1: The images show results for a single example of (a) an MR and its corresponding (d) CT image. The registration result with $\alpha = 7$ and no PCA model regularization is shown as (b) the deformed atlas CT and (e) the checkerboard fusion with the ground truth CT. Corresponding results with the usage of the prior knowledge can be seen in (c) and (f).

$\alpha = 7$ was used with and without PCA regularization. The effect is clearly

visible, especially in the facial region, when comparing the registration results with the ground truth CT. Accordingly, for the nonrigid registration without PCA regularization, a much higher value for α is used in order to regain the necessary stability. Empirically, we determined a value of $\alpha = 60$ as a good choice. Tables 1 and 2 present the results for the comparison between the two

Method	Measure				
	MSE	DistBO	SE(ST)	SE(BO)	SE(ST,BO)
No PCA	25440.8 \pm 7715.2	0.41 \pm 0.25	84.8 \pm 2.8	64.0 \pm 11.4	81.2 \pm 3.2
PCA	21297.9 \pm 10466.7	0.25 \pm 0.10	84.3 \pm 3.6	70.8 \pm 6.0	82.0 \pm 3.2

Table 1: Results for the leave-one-out cross-validation on T1-weighted MRI data. The values shown consist of the mean and the standard deviation for the corresponding measure calculated over all datasets. For mean squared error in Hounsfield units (MSE) and the distance to the bone mask in mm (DistBO), smaller values indicate better results. The sensitivity measures for segmented soft tissue (SE(ST)), bone (SE(BO)), and the combination of both (SE(ST, BO)), larger values are better.

Method	Measure				
	MSE	DistBO	SE(ST)	SE(BO)	SE(ST,BO)
No PCA	29914.7 \pm 17514.4	0.55 \pm 0.46	83.3 \pm 5.3	58.8 \pm 13.3	79.0 \pm 6.5
PCA	23966.4 \pm 10371.6	0.31 \pm 0.16	84.3 \pm 5.0	66.4 \pm 7.9	81.1 \pm 5.3

Table 2: Results for the leave-one-out cross-validation on T2-weighted MRI data. For a description of the values, see table 1.

approaches for T1- and T2-weighted MRI scans. The results of the registration are compared with the ground truth CT of the patient, who was left out for the cross-validation, based on a number of measures: The mean square error (MSE) was calculated between the intensities of both images. Since especially bone densities between different patients are usually not directly comparable, this is only a coarse measure. To compensate for these differences, the CT images are segmented into three classes for further comparisons: air, soft tissue (ST), and bone (BO). Based on these segmentations the class-specific sensitivities for soft tissue (SE(ST)), bone (SE(BO)), and the joint sensitivity (SE(ST,BO)) are calculated. A final measure (DistBO) is computed in order to provide a quantitative measure of the spatial distance between the segmentations of the bone. This measure determines the average euclidean distance between each pixel segmented as bone in one image to the nearest pixel segmented as bone in the other image. On average, the MSE measure for T1 and T2 data is decreased by

18% and the DistBO measure by 42% using the proposed algorithm. The overall sensitivity for correct soft tissue and bone alignment is increased by 4%.

5 Discussion

In this article, we have introduced a novel, PCA-based regularizing energy. This morphological term constrains the deformation to be close within the known space of variability that is learned from a training set of deformations. We have shown that this model is invariant to global translations and is able to compensate for morphologically unreasonable deformations when other regularization energies are reduced. The presented results indicate a better performance of the proposed approach with respect to especially the MSE and the distance between the bone segmentations. These two criteria are of special interest for the attenuation correction, because the location of the bones has a high impact on the corrected result. Except for the mean values of the soft tissue sensitivity, the registration with the incorporation of the prior knowledge performed better than the standard algorithm.

6 Acknowledgements

The authors would like to P. Ritt (Department of Nuclear Medicine, University Hospital, Erlangen) for his efforts in the patient data selection. We are also thankful to HipGraphics for providing the volume rendering software InSpace.

References

1. Hofmann, M., Pichler, B., Schölkopf, B., Beyer, T.: Towards quantitative pet/mri: a review of mr-based attenuation correction techniques. *European Journal of Nuclear Medicine and Molecular Imaging*, *European Journal of Nuclear Medicine and Molecular Imaging* **36**(Supplement 1) (03 2009) 93–104
2. Hofmann, M., Steinke, F., Scheel, V., Charpiat, G., Farquhar, J., Aschoff, P., Brady, M., Schölkopf, B., Pichler, B.J.: Mri-based attenuation correction for pet/mri: A novel approach combining pattern recognition and atlas registration. *Journal of Nuclear Medicine* **49**(11) (10 2008) 1875–1883
3. Wang, Y., Staib, L.H.: Physical model-based non-rigid registration incorporating statistical shape information. *Medical Image Analysis* **1** (2000) 35–51
4. Kim, M.J., Kim, M.H., Shen, D.: Learning-based deformation estimation for fast non-rigid registration. *Computer Vision and Pattern Recognition Workshop* **0** (2008) 1–6
5. Xue, Z., Shen, D.: A new statistically-constrained deformable registration framework for mr brain images. *International Journal of Medical Engineering and Informatics* **1**(3) (2009) 357 – 367
6. Hermosillo, G.: Variational Methods for Multimodal Image Matching. PhD thesis, University of Nice Sophia Antipolis, France (2002)
7. Modersitzki, J.: Numerical Methods for Image Registration. Oxford University Press, Oxford (2004)

8. Viola, P.: Alignment by Maximization of Mutual Information. PhD thesis, Massachusetts Institute of Technology (MIT), Cambridge, USA (1995)
9. Fischer, B., Modersitzki, J.: A unified approach to fast image registration and a new curvature based registration technique. *Linear Algebra and its Applications* **380** (March 2004) 107–124
10. Tikhonov, A.N., Arsenin, V.Y.: Solutions of ill posed problems. Wiley, New York (1977)
11. Shannon, C.E.: A mathematical theory of communication (parts 1 and 2). *The Bell System Technical Journal* **27** (1948) 379–423, 623–656
12. Wells III, W.M., Viola, P., Atsumi, H., Nakajima, S., Kikinis, R.: Multi-modal volume registration by maximization of mutual information. *Medical Image Analysis* **1**(1) (1996) 35–51
13. Maes, F., Collignon, A., Vandermeulen, D., Marchal, G., Suetens, P.: Multimodality image registration by maximization of mutual information. *IEEE Transactions on Medical Imaging* **16**(2) (April 1997) 187–198
14. Fischer, B., Modersitzki, J.: Curvature based image registration. *Journal of Mathematical Imaging and Vision* **18**(1) (2003) 81–85
15. Murase, W., Lindenbaum, M.: Partial eigenvalue decomposition of large images using spatial temporal adaptive method. *IEEE Transactions on Image Processing* **4**(5) (1995) 620–629